IOPscience iopscience.iop.org

Home Search Collections Journals About Contact us My IOPscience

High-frequency differential mobility in vertical transport of a confined superlattice

This article has been downloaded from IOPscience. Please scroll down to see the full text article.

1994 J. Phys.: Condens. Matter 6 10043

(http://iopscience.iop.org/0953-8984/6/46/021)

View the table of contents for this issue, or go to the journal homepage for more

Download details:
IP Address: 171.66.16.151
The article was downloaded on 12/05/2010 at 21:07

Please note that terms and conditions apply.

J. Phys.: Condens. Matter 6 (1994) 10043–10051. Printed in the UK

High-frequency differential mobility in vertical transport of a confined superlattice

X L Lei

China Centre of Advanced Science and Technology (World Laboratory), PO Box 8730, Beijing 100080, People's Republic of China, and State Key Laboratory of Functional Material for Informatics, Shanghai Institute of Metallurgy, Chinese Academy of Sciences, 865 Changning Road, Shanghai 200050, People's Republic of China

Received 4 May 1994, in final form 8 August 1994

Abstract. We report a theoretical investigation on the frequency-dependent small-signal mobility in the vertical conduction in the presence of a DC bias electric field for cylindrically confined superlattices having transverse diameters ranging from that for an extremely confined (purely one-dimensional) limit to that for an almost unconfined system. In all the cases the differential mobility exhibits peculiar frequency dependence at finite DC bias: the real part shows a broad hump before finally approaching zero at high frequency, and the imaginary part experiences a marked dip to negative values before going through the conventional maximum. Such behaviour of the frequency-dependent differential mobility stems from a decrease of the average inverse effective mass of carriers in conjunction with an increase of their average longitudinal energy, and is characterized approximately by a momentum and an energy relaxation time. It is found that the effective energy relaxation time increases significantly with increase of the transverse diameter of the superlattice.

1. Introduction

Negative differential mobility (NDM) in superlattice vertical transport, predicted more than twenty years ago by Esaki and Tsu [1], have been demonstrated experimentally [2–4]. Recent optical and coherent electromagnetic radiation measurements [5, 6] have further indicated Bloch oscillations at low temperature in superlattices with dilute carriers. These developments have not only stimulated extensive studies on the physics of these Bragg-diffraction-related phenomena [7–14] but have also introduced the prospect of developing superlattice-based microwave devices [15–17]. Although the occurrence of an oscillatory current response at Bloch frequency in high-carrier-density systems remains controversial [18], the use of a superlattice in a Gunn-like microwave device seems promising if miniband NDM can persist at sufficiently high frequency. However, the fact that Bloch miniband NDM is manifested in the drift velocity versus electric field curve under steady-state DC transport carries no assurance that it will be sustained under dynamic conditions. An early Monte Carlo study [19] seemed to indicate that NDM might persist almost up to the Bloch frequency when carrier–carrier scatterings are negligible. High carrier density and room temperature conditions are desirable for practical use of a superlattice, while strong carrier–carrier and carrier–phonon scatterings, together with the transverse motion of the carriers, may suppress the coherent Bloch oscillations [18] and destroy NDM at high frequency. Recent calculations of high-frequency small-signal response in three-dimensional (unconfined) superlattices with

0953-8984/94/4610043+09$19.50 © 1994 IOP Publishing Ltd

strong intercarrier scattering [20] indicate that differential mobility can be negative only up to a frequency lower than 100 GHz. For a confined system this frequency can be several times higher. This, together with the feasibility of reducing the heating level, makes confined superlattices advantageous for working on a NDM-related, high-frequency device.

We report here a theoretical investigation on the frequency dependence of the carrier drift velocity in miniband conduction responding to a small-signal AC electric field superimposed on a DC bias, for cylindrically confined superlattices having transverse diameters ranging from that of the extremely confined (purely one-dimensional) limit to that of the almost unconfined superlattice. We employ the balance equation theory for arbitrary energy bands [21], which is a non-parabolic extension of the Lei–Ting theory [22]. It has been used to discuss steady-state and transient transport in superlattice minibands with much success. This theory facilitates numerical calculation for an arbitrarily non-parabolic system while the role of electron heating, carrier statistics and realistic scattering mechanisms are all included. In the pure one-dimensional (1D) limit the balance equations reduce to those of Ignatov *et al* [11, 12] if the constant-relaxation-time approximation is assumed for the frictional acceleration and electron energy-loss rate. Under this approximation one can obtain the explicit analytical expression for the complex high-frequency mobility and gain physical insight into its peculiar frequency dependence more easily.

2. Equations for small-signal response

We consider a model superlattice system in which electrons can move along the z direction through the (lowest) miniband formed by the periodic potential wells and barriers of finite height. In the transverse (x–y) plane electrons either move freely in both the x and y directions (3D superlattice or unconfined superlattice) or are confined to a region by an infinitely high potential wall (1D superlattice or 2D confined superlattice).

The electron energy dispersion can be written as the sum of a transverse-motion energy $\varepsilon_{n_\parallel}$ and a tight-binding-type miniband energy $\varepsilon(k_z)$ related to the longitudinal motion:

$$\varepsilon_{n_\parallel}(k_z) = \varepsilon_{n_\parallel} + \varepsilon(k_z) \tag{1}$$

with

$$\varepsilon(k_z) = \frac{\Delta}{2}(1 - \cos k_z d) \tag{2}$$

where d is the superlattice period along the z direction, $-\pi/d < k_z \leqslant \pi/d$, and Δ is the miniband width. The electron transverse state and its energy are described by the transverse quantum number $n_\parallel$. They should be specified separately for 1D and 3D superlattices.

According to the non-parabolic balance equation theory developed by the author [21], when a time-dependent but spatially uniform electric field $E(t)$ is applied along the z direction of the superlattice, the transport state is described by the centre-of-mass (CM) momentum $P_d \equiv Np_d$ (N is the total number of carriers) and the relative electron temperature T_e, which are time-dependent parameters. The balance equations can be written as

$$\frac{dv_d}{dt} = eE/m_z^* + A_i + A_p \tag{3}$$

$$\frac{dh_e}{dt} = eEv_d - W. \tag{4}$$

Here

$$v_d = \frac{2}{N}\sum_{n_\parallel, k_z} \frac{d\varepsilon(k_z)}{dk_z} f(\varepsilon_{n_\parallel}(k_z - p_d), T_e) \tag{5}$$

is the centre-of-mass velocity, or the average drift velocity of the carrier in the z direction,

$$\frac{1}{m_z^*} = \frac{2}{N}\sum_{n_\parallel,k_z} \frac{\mathrm{d}^2\varepsilon(k_z)}{dk_z^2} f(\varepsilon_{n_\parallel}(k_z - p_\mathrm{d}), T_\mathrm{e}) \tag{6}$$

is the averaged inverse effective mass of the CM, and

$$h_\mathrm{e} = \frac{2}{N}\sum_{n_\parallel,k_z} \varepsilon_{n_\parallel}(k_z) f(\varepsilon_{n_\parallel}(k_z - p_\mathrm{d}), T_\mathrm{e}) \tag{7}$$

is the average electron energy per carrier. In these equations

$$f(\varepsilon, T_\mathrm{e}) \equiv \{\exp[(\varepsilon - \mu)/T_\mathrm{e}] + 1\}^{-1}$$

stands for the Fermi distribution function at the electron temperature T_e, and μ is the chemical potential determined by the condition that the total number of electrons equals N:

$$N = 2\sum_{n_\parallel,k_z} f(\varepsilon_{n_\parallel}(k_z), T_\mathrm{e}). \tag{8}$$

The expressions for the impurity- and phonon-induced frictional accelerations, A_i and A_p, and the energy transfer rate from the electron system to the phonon system, W, have been given in [7] and [10] respectively for 3D and 1D superlattices, together with the form factors due to longitudinal and transverse wavefunctions.

With the miniband energy dispersion of (1), the average electron energy is the sum of an average transverse energy

$$\epsilon_\parallel = \frac{2}{N}\sum_{n_\parallel,k_z} \varepsilon_{n_\parallel} f(\varepsilon_{n_\parallel}(k_z - p_\mathrm{d}), T_\mathrm{e}) \tag{9}$$

and an average longitudinal energy ϵ_z

$$\epsilon_z = \frac{2}{N}\sum_{n_\parallel,k_z} \varepsilon(k_z) f(\varepsilon_{n_\parallel}(k_z - p_\mathrm{d}), T_\mathrm{e}) = (\Delta/2)[1 - \alpha(T_\mathrm{e})\cos(z_\mathrm{d})]. \tag{10}$$

The drift velocity is given by

$$v_\mathrm{d} = v_m \alpha(T_\mathrm{e}) \sin(z_\mathrm{d}) \tag{11}$$

and the ensemble-averaged inverse effective mass turns out to be a function of ϵ_z only:

$$m_z^* \equiv m_z^*(\epsilon_z) = M^*/(1 - 2\epsilon_z/\Delta). \tag{12}$$

Here $v_m = \Delta d/2$, $1/M^* = \Delta d^2/2$, and

$$\alpha(T_\mathrm{e}) = \frac{2}{N}\sum_{n_\parallel,k_z} \cos(k_z d) f(\varepsilon_{n_\parallel}(k_z), T_\mathrm{e}) \tag{13}$$

is a function of T_e, independent of $z_\mathrm{d} \equiv p_\mathrm{d} d$.

Consider that a DC bias electric field E_0 and a small-signal AC electric field δE of single frequency ω are applied along the superlattice axis:

$$E(t) = E_0 + \delta E. \tag{14}$$

After a transient process, the system reaches a steady state in which z_d, T_e can be written in terms of a DC bias part and a small AC response: $z_\mathrm{d} = z_0 + \delta z$, $T_\mathrm{e} = T_0 + \delta T$, and all other quantities in the balance equations can be expanded to linear order in the small AC quantities about the bias point z_0 and T_0. For zeroth order we have just the DC steady-state equations:

$$0 = edE_0\alpha_0 \cos(z_0) + 2A_0/(\Delta d) \tag{15}$$

$$0 = edE_0\alpha_0 \sin(z_0) - 2W_0/\Delta \tag{16}$$

where we write $\alpha_0 \equiv \alpha(T_0)$, $A_0 \equiv A(z_0, T_0)$ and $W_0 \equiv W(z_0, T_0)$. These two equations determine z_0, T_0 and thus the DC drift velocity at the the bias point: $v_0 = v_m\alpha_0 \sin(z_0)$. The equations for linear-order AC quantities are as follows:

$$\alpha_0 \cos(z_0)\frac{\mathrm{d}}{\mathrm{d}t}(\delta z) + \alpha_0' \sin(z_0)\frac{\mathrm{d}}{\mathrm{d}t}(\delta T)$$
$$= ed\alpha_0 \cos(z_0)\,\delta E + \left[-edE_0\alpha_0 \sin(z_0) + \frac{2}{\Delta d}\left(\frac{\partial A_0}{\partial z_\mathrm{d}}\right)\right]\delta z$$
$$+ \left[edE_0\alpha_0' \cos(z_0) + \frac{2}{\Delta d}\left(\frac{\partial A_0}{\partial T_\mathrm{e}}\right)\right]\delta T \tag{17}$$

$$\alpha_0 \sin(z_0)\frac{\mathrm{d}}{\mathrm{d}t}(\delta z) - \left[\alpha_0' \cos(z_0) - 2\epsilon_{\|0}'/\Delta\right]\frac{\mathrm{d}}{\mathrm{d}t}(\delta T)$$
$$= ed\alpha_0 \sin(z_0)\,\delta E + \left[edE_0\alpha_0 \cos(z_0) - \frac{2}{\Delta}\left(\frac{\partial W_0}{\partial z_\mathrm{d}}\right)\right]\delta z$$
$$+ \left[edE_0\alpha_0' \sin(z_0) - \frac{2}{\Delta d}\left(\frac{\partial W_0}{\partial T_\mathrm{e}}\right)\right]\delta T. \tag{18}$$

Here we have used the symbols $\alpha_0' \equiv \mathrm{d}\alpha(T_0)/\mathrm{d}T_\mathrm{e}$ and $\epsilon_{\|0}' \equiv \mathrm{d}\epsilon_\|(z_0, T_0)/\mathrm{d}T_\mathrm{e}$. This set of equations linear in small AC quantities is conveniently solved for a single-frequency driving field by using a complex form: $\delta E = E_1\mathrm{e}^{-\mathrm{i}\omega t}$. For the AC steady state, δz and δT oscillate at the same single frequency: $\delta z = z_1\mathrm{e}^{-\mathrm{i}\omega t}$ and $\delta T = T_1\mathrm{e}^{-\mathrm{i}\omega t}$, leading to an oscillating AC drift velocity given by $\delta v = v_1\mathrm{e}^{-\mathrm{i}\omega t}$, superposed on the DC drift velocity, with

$$v_1 = v_m\left[\alpha_0 \cos(z_0)z_1 + \alpha_0' \sin(z_0)T_1\right]. \tag{19}$$

The complex frequency-dependent mobility is defined as

$$\mu_\omega = v_1/E_1. \tag{20}$$

3. Pure 1D case; relaxation time approximation

Considering the case in which the carriers are confined to very small dimensions in both directions in the lateral plane (1D superlattice) such that they are frozen in the lowest lateral subband, the balance equations (3) and (4) become

$$\mathrm{d}v_\mathrm{d}/\mathrm{d}t = eE/m_z^*(\epsilon_z) + A \tag{21}$$

$$\mathrm{d}\epsilon_z/\mathrm{d}t = eEv_\mathrm{d} - W. \tag{22}$$

Equations (21) and (22), in the constant-relaxation-time form, have been used by Ignatov *et al* [11, 12] to discuss steady-state, transient and high-frequency transport in the superlattice miniband. The constant-relaxation-time approximation assumes that the *frictional acceleration* $A = A_\mathrm{i} + A_\mathrm{p}$ *is proportional to the drift velocity:*

$$A = -v_\mathrm{d}/\tau \tag{23}$$

(τ is called the momentum relaxation time) and the energy transfer rate W is proportional to the energy deviation from the equilibrium value ϵ_T at the lattice temperature T in the absence of the electric field:

$$W = (\epsilon_z - \epsilon_T)/\tau_\epsilon \tag{24}$$

(τ_ε is called the energy relaxation time). Here the equilibrium energy ϵ_T, given by

$$\epsilon_T = \frac{2}{N}\sum_{n_\parallel,k_z} \varepsilon(k_z) f(\varepsilon_{n_\parallel}(k_z), T) = (\Delta/2)[1-\alpha(T)] \tag{25}$$

and is different from what was used by Ignatov *et al* [11, 12]:

$$\epsilon_T = \frac{\Delta}{2}\left[1 - \frac{I_1(\Delta/2T)}{I_0(\Delta/2T}\right]. \tag{26}$$

If the electron system is in a non-degenerate limit, $-\mu/T \gg 1$, the present ϵ_T (equation (25)) reduces to Ignatov's ϵ_T (equation (26)). Unfortunately, in such a purely one-dimensional system the non-degenerate limit does not generally exist [10] no matter how high the temperature is, except for in the case of very small electron density $N_1 d \sim 0$ such that $\ln(2/N_1 d - 1) \gg 1$. Therefore the expression (26) can only describe a very dilute electron system at high temperatures. In general, it should be replaced by (25).

When a DC bias electric field E_0 and a small-AC-signal electric field of single frequency, $\delta E = E_1 e^{-i\omega t}$, are applied, one can write $v_d = v_0 + \delta v$ and $\epsilon_z = \epsilon_0 + \delta\epsilon$, and balance equations (21) and (22) yield a bias drift velocity v_0 given by

$$v_0 = 2v_p \frac{b}{1+b^2} \tag{27}$$

where $b \equiv E_0/E_c$, with

$$E_c = 1/[ed(\tau\tau_\varepsilon)^{1/2}] \tag{28}$$

and

$$v_p = \frac{\Delta d}{4}\left(\frac{\tau}{\tau_\varepsilon}\right)^{1/2}\alpha(T). \tag{29}$$

These expressions were given by Ignatov *et al* [11, 12], except that there $\alpha(T)$ is replaced by $I_1(\Delta/2T)/I_0(\Delta/2T)$. The first order equations for small-signal response read

$$\frac{d}{dt}\delta v + \frac{\delta v}{\tau} = \frac{e\,\delta E}{m_z^*(\epsilon_0)} - eE_0 d^2\,\delta\epsilon \tag{30}$$

$$\frac{d}{dt}\delta\epsilon + \frac{\delta\epsilon}{\tau_\varepsilon} = ev_0\,\delta E + eE_0\,\delta v. \tag{31}$$

The second term on the right-hand side of (30) comes from the fact that the increase in the system internal energy, $\delta\epsilon$, due to a small increment of the signal field results in a decrease in the inverse effective mass. This effect has a profound influence on the differential mobility. In fact, the above equations yield a differential mobility at frequency ω of the form

$$\mu_\omega = \frac{e\tau}{m_z^*(\epsilon_0)}\frac{1 - b^2(1-i\omega\tau_\varepsilon)^{-1}}{1 - i\omega\tau + b^2(1-i\omega\tau_\varepsilon)^{-1}}. \tag{32}$$

The zero-frequency differential mobility is given by

$$\mu_0 = \frac{e\tau}{m_z^*(\epsilon_0)}\frac{1-b^2}{1+b^2}. \tag{33}$$

The terms containing b^2 are related to the second term on the right-hand side of (30). We can see that when a small AC field δE is applied together with a finite DC bias $E_0 \neq 0$, there are two influential effects. First, at finite bias field E_0 the inverse effective mass $1/m_z^*(\varepsilon_0)$ is smaller than at zero bias, and it decreases monotonically with increasing E_0 because the average longitudinal energy ϵ_0 increases. However, since $1/m_z^*(\epsilon_0)$, determined

by the steady-state DC balance equations, is always positive, this effect, though tending to decrease the differential mobility, cannot bring it into the negative regime. The occurrence of negative differential mobility devolves upon the fact that a positive δE induces a positive $\delta\epsilon$, as required by the energy balance equation, and this $\delta\epsilon$ in turn results in an additional negative change of the inverse effective mass, which contributes a negative term (the term containing b^2 in the numerator of (30)) to the differential mobility at a non-zero DC bias. *It is just this contribution that gives rise to negative differential mobility at low frequency* in superlattice miniband transport. This effect, which stems from the change of average longitudinal energy with a small AC electric field signal, however, is frequency dependent. At higher frequency, when $\delta\epsilon$ cannot synchronously follow δE as in the zero-frequency limit, this effect weakens and consequently $\mathrm{Re}\,\mu_\omega$ may exhibit an increase with increasing frequency at finite DC bias. Figure 1 shows the real part of μ_ω as a function of frequency at bias DC field $b \equiv E_0/E_c = 0$, 0.1, 0.3, 0.5, 1, 1.7, 3, 5, 10 and 20, for the case of $\tau_\epsilon = 10\tau$. It is just this effect that gives rise to the humps in Re μ_ω as a function of $\omega\tau$ before it finally vanishes at large $\omega\tau$. Without this effect (i.e. $b = 0$ and thus $\epsilon_0 = \epsilon_T$) μ_ω will take Drude form:

$$\mu_\omega = \frac{\mu_0(0)}{1 - \mathrm{i}\omega\tau} \tag{34}$$

in which

$$\mu_0(0) = \frac{e\tau}{m_z^*(\epsilon_T)} = \frac{1}{2}\Delta d^2\, e\tau\alpha(T) \tag{35}$$

is the zero-frequency mobility at zero DC bias.

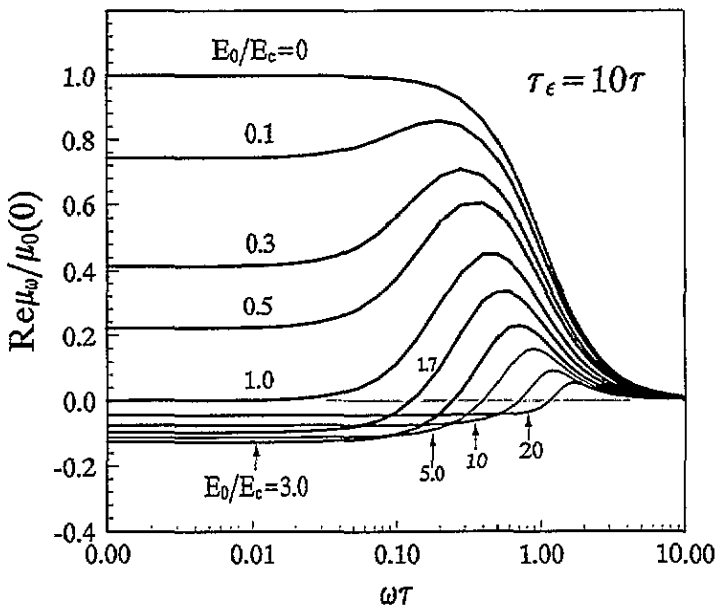

Figure 1. The real part of the frequency-dependent mobility μ_ω, as predicted by (32) in the case of $\tau_\epsilon = 10\tau$, is shown as a function of $\omega\tau$ for different bias DC fields.

4. 3D systems; realistic scatterings

Apparently, the constant-relaxation-time approximation for the frictional acceleration A and the energy-loss rate W is difficult to justify for a real system. To go beyond this approximation and to take account of the realistic impurity and phonon scatterings, we return to (15) and (16), and (17) and (18). We consider a cylindrically confined GaAs-based quantum well superlattice, in which electrons are assumed to be confined to a small cylindrical region of diameter d_r by an infinitely high potential wall. The transverse quantum number $n_\parallel = (l, n)$ ($l = 1, 2, \ldots$ and $n = 0, \pm 1, \pm 2, \ldots$), and the transverse energy of the electron state is given by

$$\varepsilon_{n_\parallel} = 2(x_l^n)^2/(md_r^2) \tag{36}$$

where m is the electron band effective mass of the background bulk material, and x_l^n represents the lth zero of the nth-order Bessel function, i.e. $J_n(x_l^n) = 0$.

We include electron scatterings from randomly distributed impurities, longitudinal and transverse acoustic phonons (through deformation potential and piezoelectric couplings with electrons) and polar optic phonons (through Fröhlich coupling with electrons). The detailed description of these couplings and the form factors appearing in the expressions for A and W has been given elsewhere [10]. All the parameters used in the calculations are typical values of GaAs.

For extremely confined systems, e.g. for $d_r \leqslant 10\,\text{nm}$, it is a good approximation to consider the lowest subband and we have a purely 1D system. The term containing the transverse energy $\epsilon'_{\parallel 0}$ in (18) disappears and (15)–(18) are readily solved to obtain the complex frequency-dependent mobility, limited by realistic scatterings. The numerical results for both $\text{Re}\,\mu_\omega$ and $\text{Im}\,\mu_\omega$ are qualitatively quite similar to those obtained from purely 1D equations with the relaxation time approximation.

With increasing cylindrical diameter of the 1D superlattice, the influence of the carrier transverse movement begins to emerge, and the occupation of many subbands has to be taken into account. To see how the cylindrical diameter affects the frequency-dependent mobility, we have calculated the real part $\text{Re}\,\mu_\omega$ and the imaginary part $\text{Im}\,\mu_\omega$ of the frequency-dependent differential mobility μ_ω from equations (15) to (18) at lattice temperature $T = 300\,\text{K}$, for several superlattices having period $d = 10\,\text{nm}$, miniband width $\Delta = 900\,\text{K}$, and low-temperature linear mobility $\mu(0) = 1.0\,\text{m}^2\,\text{V}^{-1}\,\text{s}^{-1}$, but with cylindrical diameter d_r varying from 20 nm to 40 nm, and carrier line density $N_1 d$ equal to $nd(\pi d_r^2/4)$, which is chosen separately for each d_r such that the equivalent 3D densities n are kept the same, $n = 6.75\times 10^{24}\,\text{m}^3$, for all systems. As many as 21 transverse subbands are considered in the calculation. To save space we only plot the numerical results for the system of $d_r = 40\,\text{nm}$ in figure 2. The linear mobility of this system is $0.545\,\text{m}^2\,\text{V}^{-1}\,\text{s}^{-1}$ at $T = 300\,\text{K}$. If one still tries to characterize the frequency dependence of μ_ω qualitatively in terms of the above two-relaxation-time model as given by (32), the main effect of increasing the transverse diameter from $d_r = 10\,\text{nm}$ to $d_r = 40\,\text{nm}$ appears to be the increase in the effective energy relaxation time τ_ε: approximately 0.35 ps for the $d_r = 10\,\text{nm}$ system and 2.3 ps for the $d_r = 40\,\text{nm}$ system. The effective momentum relaxation time τ also changes from about 0.08 ps for the $d_r = 10\,\text{nm}$ system to about 0.15 ps for the $d_r = 40\,\text{nm}$ system.

5. Discussion

We have presented a theoretical investigation on the high-frequency small-signal mobility in the presence of a DC bias for laterally confined superlattices. To concentrate on the pure

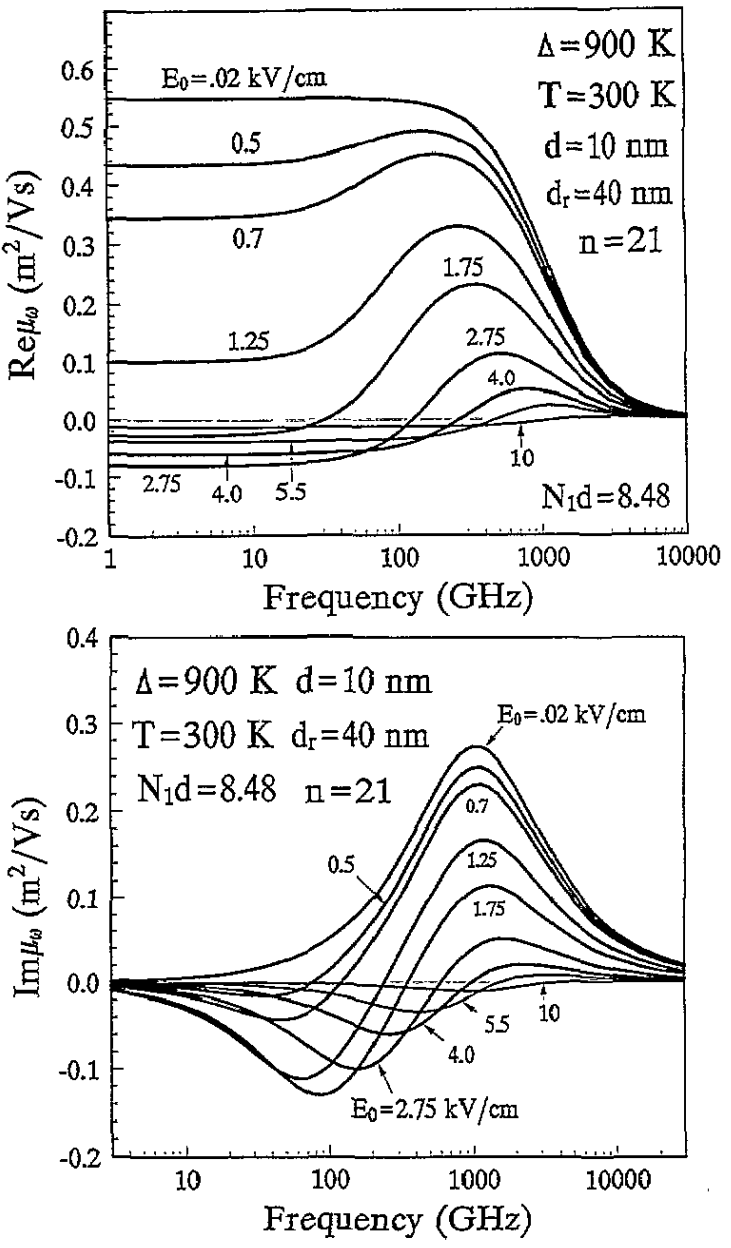

Figure 2. The real part, $\mathrm{Re}\,\mu_\omega$, and the imaginary part, $\mathrm{Im}\,\mu_\omega$, of the frequency-dependent mobility are plotted against the signal frequency $\nu = \omega/2\pi$ at several different DC bias fields E_0 and at lattice temperature $T = 300\,\mathrm{K}$, for a GaAs-based cylindrically confined superlattice with traverse diameter $d_r = 40\,\mathrm{nm}$, period $d = 10\,\mathrm{nm}$, miniband width $\Delta = 900\,\mathrm{K}$, electron density $N_1 d = 8.48$ and low-temperature linear DC mobility $\mu(0) = 1.0\,\mathrm{m^2\ V^{-1}\ s^{-1}}$. The numerical calculations were carried using (15)–(18), considering the 21 lowest transverse subbands.

superlattice effect we have used an idealized model without intersubband (Zener) tunnelling, intervalley (Γ–X) scattering, higher miniband occupation, and many other processes that may occur in actual systems. Such an idealized model does represent the main physics of an experimentally carefully devised system under appropriate conditions. The present balance

equation analysis provided a physical insight into the NDM for high frequency and allowed us to calculate the frequency-dependent current response of the system, without considering the spatial inhomogeneity. Exploring the formation and the motion of electron wave packets or domains from a space- and time-dependent set of equations is, of course, highly desirable and will be the subject of a future study. Nevertheless, the present homogeneous treatment sets an upper limit for the frequency attainable in a superlattice-based NDM device and constitutes a first step toward an inhomogeneous analysis.

Acknowledgments

The author wishes to thank Drs N J M Horing and H L Cui for helpful discussions. This work was supported by the National Natural Science Foundation of China and by the National and Shanghai Municipal Commissions of Science and Technology of China.

References

[1] Esaki L and Tsu R 1970 *IBM J. Res. Dev.* **14** 61
[2] Sibille A, Palmier J F, Wang H and Mollot F 1990 *Phys. Rev. Lett.* **64** 52
[3] Beltram F, Capasso F, Sivco D L, Hutchinson A L and Chu S N G 1990 *Phys. Rev. Lett.* **64** 3167
[4] Grahn H T, von Klitzing K, Ploog K and Döhler G H 1991 *Phys. Rev.* B **43** 12 094
[5] Feldmann J, Leo K, Shah J, Miller D A B, Cunningham J E, Meier T, von Plessen G, Schulze A, Thomas P and Schmitt-Rink S 1992 *Phys. Rev.* B **46** 7252
Leo K, Bolivar P H, Brüggemann F, Schwedler R and Köhler K 1992 *Solid State Commun.* **84** 943
[6] Waschke C, Roskos H G, Schwedler R, Leo K, Kurz H and Köhler K 1993 *Phys. Rev. Lett.* **70** 3319
[7] Lei X L, Horing N J M and Cui H L 1991 *Phys. Rev. Lett.* **66** 3277; 1992 *J. Phys.: Condens. Matter* **4** 9375
[8] Lei X L and da Cunha Lima I C 1992 *J. Appl. Phys.* **71** 5517
[9] Lei X L 1992 *J. Phys.: Condens. Matter* **4** L659
[10] Lei X L 1992 *J. Phys.: Condens. Matter* **4** 9367
Lei X L and Wang X F 1993 *J. Appl. Phys.* **73** 3867
[11] Ignatov A A, Dodin E P and Shashkin V I 1991 *Mod. Phys. Lett* B **5** 1087
[12] Ignatov A A, Renk K F and Dodin E P 1993 *Phys. Rev. Lett.* **70** 1996
[13] Gerhardts R R 1993 *Phys. Rev.* B **48** 9178
[14] Palmier J F *et al* 1993 *Proc. 6th Int. Conf. on Modulated Semiconductor Structures (Garmish-Partenkirchen, Germany 1993)*
[15] Hadjazi M, Sibille A, Palmier P J and Mollot F 1992 *Electron. Lett.* **27** 1101
[16] Sibille A 1993 *Superlatt. Microstruct.* **13** 247
[17] Lei X L, Horing N J M, Cui H L and Thornber K K 1993 *Phys. Rev.* B **48** 5366; 1993 *Solid State Commun.* **86** 231
[18] Lei X L 1994 *J. Phys.: Condens. Matter* **6** 3749; 1994 *Semicond. Sci. Technol.* **9** 567
[19] Price P J 1973 *IBM. J. Res. Dev.* **17** 39
[20] Lei X L, Horing N J M, Cui H L and Thornber K K 1994 to be published
[21] Lei X L 1992 *Phys. Status Solidi* b **170** 519
[22] Lei X L and Ting C S 1984 *Phys. Rev.* B **30** 4809; 1985 *Phys. Rev.* B **32** 1112